

Search for Lepton Flavor Violating Decays $\tau^- \rightarrow l^- K_s^0$ with the BABAR Experiment

B. Aubert,¹ M. Bona,¹ Y. Karyotakis,¹ J. P. Lees,¹ V. Poireau,¹ E. Prencipe,¹ X. Prudent,¹ V. Tisserand,¹ J. Garra Tico,² E. Grauges,² L. Lopez,^{3a,3b} A. Palano,^{3a,3b} M. Pappagallo,^{3a,3b} G. Eigen,⁴ B. Stugu,⁴ L. Sun,⁴ G. S. Abrams,⁵ M. Battaglia,⁵ D. N. Brown,⁵ R. N. Cahn,⁵ R. G. Jacobsen,⁵ L. T. Kerth,⁵ Yu. G. Kolomensky,⁵ G. Lynch,⁵ I. L. Osipenkov,⁵ M. T. Ronan,^{5,*} K. Tackmann,⁵ T. Tanabe,⁵ C. M. Hawkes,⁶ N. Soni,⁶ A. T. Watson,⁶ H. Koch,⁷ T. Schroeder,⁷ D. Walker,⁸ D. J. Asgeirsson,⁹ B. G. Fulsom,⁹ C. Hearty,⁹ T. S. Mattison,⁹ J. A. McKenna,⁹ M. Barrett,¹⁰ A. Khan,¹⁰ V. E. Blinov,¹¹ A. D. Bukin,¹¹ A. R. Buzykaev,¹¹ V. P. Druzhinin,¹¹ V. B. Golubev,¹¹ A. P. Onuchin,¹¹ S. I. Serednyakov,¹¹ Yu. I. Skovpen,¹¹ E. P. Solodov,¹¹ K. Yu. Todyshev,¹¹ M. Bondioli,¹² S. Curry,¹² I. Eschrich,¹² D. Kirkby,¹² A. J. Lankford,¹² P. Lund,¹² M. Mandelkern,¹² E. C. Martin,¹² D. P. Stoker,¹² S. Abachi,¹³ C. Buchanan,¹³ J. W. Gary,¹⁴ F. Liu,¹⁴ O. Long,¹⁴ G. M. Vitug,¹⁴ Z. Yasin,¹⁴ L. Zhang,¹⁴ V. Sharma,¹⁵ C. Campagnari,¹⁶ T. M. Hong,¹⁶ D. Kovalskiy,¹⁶ M. A. Mazur,¹⁶ J. D. Richman,¹⁶ T. W. Beck,¹⁷ A. M. Eisner,¹⁷ C. J. Flacco,¹⁷ C. A. Heusch,¹⁷ J. Kroseberg,¹⁷ W. S. Lockman,¹⁷ A. J. Martinez,¹⁷ T. Schalk,¹⁷ B. A. Schumm,¹⁷ A. Seiden,¹⁷ M. G. Wilson,¹⁷ L. O. Winstrom,¹⁷ C. H. Cheng,¹⁸ D. A. Doll,¹⁸ B. Echenard,¹⁸ F. Fang,¹⁸ D. G. Hitlin,¹⁸ I. Narsky,¹⁸ T. Piatenko,¹⁸ F. C. Porter,¹⁸ R. Andreassen,¹⁹ G. Mancinelli,¹⁹ B. T. Meadows,¹⁹ K. Mishra,¹⁹ M. D. Sokoloff,¹⁹ P. C. Bloom,²⁰ W. T. Ford,²⁰ A. Gaz,²⁰ J. F. Hirschauer,²⁰ M. Nagel,²⁰ U. Nauenberg,²⁰ J. G. Smith,²⁰ K. A. Ulmer,²⁰ S. R. Wagner,²⁰ R. Ayad,^{21,†} A. Soffer,^{21,‡} W. H. Toki,²¹ R. J. Wilson,²¹ E. Feltresi,²² A. Hauke,²² H. Jasper,²² M. Karbach,²² J. Merkel,²² A. Petzold,²² B. Spaan,²² K. Wacker,²² M. J. Kobel,²³ R. Nogowski,²³ K. R. Schubert,²³ R. Schwierz,²³ A. Volk,²³ D. Bernard,²⁴ G. R. Bonneaud,²⁴ E. Latour,²⁴ M. Verderi,²⁴ P. J. Clark,²⁵ S. Playfer,²⁵ J. E. Watson,²⁵ M. Andreotti,^{26a,26b} D. Bettoni,^{26a} C. Bozzi,^{26a} R. Calabrese,^{26a,26b} A. Cecchi,^{26a,26b} G. Cibinetto,^{26a,26b} P. Franchini,^{26a,26b} E. Luppi,^{26a,26b} M. Negrini,^{26a,26b} A. Petrella,^{26a,26b} L. Piemontese,^{26a} V. Santoro,^{26a,26b} R. Baldini-Ferroli,²⁷ A. Calcaterra,²⁷ R. de Sangro,²⁷ G. Finocchiaro,²⁷ S. Pacetti,²⁷ P. Patteri,²⁷ I. M. Peruzzi,^{27,§} M. Piccolo,²⁷ M. Rama,²⁷ A. Zallo,²⁷ A. Buzzo,^{28a} R. Contri,^{28a,28b} M. Lo Vetere,^{28a,28b} M. M. Macri,^{28a} M. R. Monge,^{28a,28b} S. Passaggio,^{28a} C. Patrignani,^{28a,28b} E. Robutti,^{28a} A. Santroni,^{28a,28b} S. Tosi,^{28a,28b} K. S. Chaisanguanthum,²⁹ M. Morii,²⁹ A. Adametz,³⁰ J. Marks,³⁰ S. Schenk,³⁰ U. Uwer,³⁰ V. Klose,³¹ H. M. Lacker,³¹ D. J. Bard,³² P. D. Dauncey,³² J. A. Nash,³² M. Tibbetts,³² P. K. Behera,³³ X. Chai,³³ M. J. Charles,³³ U. Mallik,³³ J. Cochran,³⁴ H. B. Crawley,³⁴ L. Dong,³⁴ W. T. Meyer,³⁴ S. Prell,³⁴ E. I. Rosenberg,³⁴ A. E. Rubin,³⁴ Y. Y. Gao,³⁵ A. V. Gritsan,³⁵ Z. J. Guo,³⁵ C. K. Lae,³⁵ N. Arnaud,³⁶ J. Béquilleux,³⁶ A. D'Orazio,³⁶ M. Davier,³⁶ J. Firmino da Costa,³⁶ G. Grosdidier,³⁶ A. Höcker,³⁶ F. Le Diberder,³⁶ V. Lepeltier,³⁶ A. M. Lutz,³⁶ S. Pruvot,³⁶ P. Roudeau,³⁶ M. H. Schune,³⁶ J. Serrano,³⁶ V. Sordini,^{36,||} A. Stocchi,³⁶ G. Wormser,³⁶ D. J. Lange,³⁷ D. M. Wright,³⁷ I. Bingham,³⁸ J. P. Burke,³⁸ C. A. Chavez,³⁸ J. R. Fry,³⁸ E. Gabathuler,³⁸ R. Gamet,³⁸ D. E. Hutchcroft,³⁸ D. J. Payne,³⁸ C. Touramanis,³⁸ A. J. Bevan,³⁹ C. K. Clarke,³⁹ K. A. George,³⁹ F. Di Lodovico,³⁹ R. Sacco,³⁹ M. Sigamani,³⁹ G. Cowan,⁴⁰ H. U. Flaecher,⁴⁰ D. A. Hopkins,⁴⁰ S. Paramesvaran,⁴⁰ F. Salvatore,⁴⁰ A. C. Wren,⁴⁰ D. N. Brown,⁴¹ C. L. Davis,⁴¹ A. G. Denig,⁴² M. Fritsch,⁴² W. Gradl,⁴² G. Schott,⁴² K. E. Alwyn,⁴³ D. Bailey,⁴³ R. J. Barlow,⁴³ Y. M. Chia,⁴³ C. L. Edgar,⁴³ G. Jackson,⁴³ G. D. Lafferty,⁴³ T. J. West,⁴³ J. I. Yi,⁴³ J. Anderson,⁴⁴ C. Chen,⁴⁴ A. Jawahery,⁴⁴ D. A. Roberts,⁴⁴ G. Simi,⁴⁴ J. M. Tuggle,⁴⁴ C. Dallapiccola,⁴⁵ X. Li,⁴⁵ E. Salvati,⁴⁵ S. Saremi,⁴⁵ R. Cowan,⁴⁶ D. Dujmic,⁴⁶ P. H. Fisher,⁴⁶ S. W. Henderson,⁴⁶ G. Sciolla,⁴⁶ M. Spitznagel,⁴⁶ F. Taylor,⁴⁶ R. K. Yamamoto,⁴⁶ M. Zhao,⁴⁶ P. M. Patel,⁴⁷ S. H. Robertson,⁴⁷ A. Lazzaro,^{48a,48b} V. Lombardo,^{48a} F. Palombo,^{48a,48b} J. M. Bauer,⁴⁹ L. Cremaldi,⁴⁹ R. Godang,^{49,¶} R. Kroeger,⁴⁹ D. A. Sanders,⁴⁹ D. J. Summers,⁴⁹ H. W. Zhao,⁴⁹ M. Simard,⁵⁰ P. Taras,⁵⁰ F. B. Viaud,⁵⁰ H. Nicholson,⁵¹ G. De Nardo,^{52a,52b} L. Lista,^{52a} D. Monorchio,^{52a,52b} G. Onorato,^{52a,52b} C. Sciacca,^{52a,52b} G. Raven,⁵³ H. L. Snoek,⁵³ C. P. Jessop,⁵⁴ K. J. Knoepfel,⁵⁴ J. M. LoSecco,⁵⁴ W. F. Wang,⁵⁴ G. Benelli,⁵⁵ L. A. Corwin,⁵⁵ K. Honscheid,⁵⁵ H. Kagan,⁵⁵ R. Kass,⁵⁵ J. P. Morris,⁵⁵ A. M. Rahimi,⁵⁵ J. J. Regensburger,⁵⁵ S. J. Sekula,⁵⁵ Q. K. Wong,⁵⁵ N. L. Blount,⁵⁶ J. Brau,⁵⁶ R. Frey,⁵⁶ O. Igonkina,⁵⁶ J. A. Kolb,⁵⁶ M. Lu,⁵⁶ R. Rahmat,⁵⁶ N. B. Sinev,⁵⁶ D. Strom,⁵⁶ J. Strube,⁵⁶ E. Torrence,⁵⁶ G. Castelli,^{57a,57b} N. Gagliardi,^{57a,57b} M. Margoni,^{57a,57b} M. Morandin,^{57a} M. Posocco,^{57a} M. Rotondo,^{57a} F. Simonetto,^{57a,57b} R. Stroili,^{57a,57b} C. Voci,^{57a,57b} P. del Amo Sanchez,⁵⁸ E. Ben-Haim,⁵⁸ H. Briand,⁵⁸ G. Calderini,⁵⁸ J. Chauveau,⁵⁸ P. David,⁵⁸ L. Del Buono,⁵⁸ O. Hamon,⁵⁸ Ph. Leruste,⁵⁸ J. Ocariz,⁵⁸ A. Perez,⁵⁸ J. Prendki,⁵⁸ S. Sitt,⁵⁸ L. Gladney,⁵⁹ M. Biasini,^{60a,60b} R. Covarelli,^{60a,60b} E. Manoni,^{60a,60b} C. Angelini,^{61a,61b} G. Batignani,^{61a,61b} S. Bettarini,^{61a,61b} M. Carpinelli,^{61a,61b,**} A. Cervelli,^{61a,61b} F. Forti,^{61a,61b} M. A. Giorgi,^{61a,61b} A. Lusiani,^{61a,61c} G. Marchiori,^{61a,61b} M. Morganti,^{61a,61b} N. Neri,^{61a,61b} E. Paoloni,^{61a,61b} G. Rizzo,^{61a,61b} J. J. Walsh,^{61a} D. Lopes Pegna,¹ C. Lu,¹ J. Olsen,¹ A. J. S. Smith,¹ A. V. Telnov,¹ F. Anulli,^{63a} E. Baracchini,^{63a,63b} G. Cavoto,^{63a} D. del Re,^{63a,63b} E. Di Marco,^{63a,63b} R. Faccini,^{63a,63b} F. Ferrarotto,^{63a} F. Ferroni,^{63a,63b} M. Gaspero,^{63a,63b} P. D. Jackson,^{63a} L. Li Gioi,^{63a} M. A. Mazzoni,^{63a} S. Morganti,^{63a}

G. Piredda,^{63a} F. Polci,^{63a,63b} F. Renga,^{63a,63b} C. Voena,^{63a} M. Ebert,⁶⁴ T. Hartmann,⁶⁴ H. Schröder,⁶⁴ R. Waldi,⁶⁴ T. Adye,⁶⁵ B. Franek,⁶⁵ E. O. Olaiya,⁶⁵ F. F. Wilson,⁶⁵ S. Emery,⁶⁶ M. Escalier,⁶⁶ L. Esteve,⁶⁶ S. F. Ganzhur,⁶⁶ G. Hamel de Monchenault,⁶⁶ W. Kozanecki,⁶⁶ G. Vasseur,⁶⁶ Ch. Yèche,⁶⁶ M. Zito,⁶⁶ X. R. Chen,⁶⁷ H. Liu,⁶⁷ W. Park,⁶⁷ M. V. Purohit,⁶⁷ R. M. White,⁶⁷ J. R. Wilson,⁶⁷ M. T. Allen,⁶⁸ D. Aston,⁶⁸ R. Bartoldus,⁶⁸ P. Bechtle,⁶⁸ J. F. Benitez,⁶⁸ R. Cenci,⁶⁸ J. P. Coleman,⁶⁸ M. R. Convery,⁶⁸ J. C. Dingfelder,⁶⁸ J. Dorfan,⁶⁸ G. P. Dubois-Felsmann,⁶⁸ W. Dunwoodie,⁶⁸ R. C. Field,⁶⁸ A. M. Gabareen,⁶⁸ S. J. Gowdy,⁶⁸ M. T. Graham,⁶⁸ P. Grenier,⁶⁸ C. Hast,⁶⁸ W. R. Innes,⁶⁸ J. Kaminski,⁶⁸ M. H. Kelsey,⁶⁸ H. Kim,⁶⁸ P. Kim,⁶⁸ M. L. Kocian,⁶⁸ D. W. G. S. Leith,⁶⁸ S. Li,⁶⁸ B. Lindquist,⁶⁸ S. Luitz,⁶⁸ V. Luth,⁶⁸ H. L. Lynch,⁶⁸ D. B. MacFarlane,⁶⁸ H. Marsiske,⁶⁸ R. Messner,⁶⁸ D. R. Muller,⁶⁸ H. Neal,⁶⁸ S. Nelson,⁶⁸ C. P. O'Grady,⁶⁸ I. Ofte,⁶⁸ A. Perazzo,⁶⁸ M. Perl,⁶⁸ B. N. Ratcliff,⁶⁸ A. Roodman,⁶⁸ A. A. Salnikov,⁶⁸ R. H. Schindler,⁶⁸ J. Schwiening,⁶⁸ A. Snyder,⁶⁸ D. Su,⁶⁸ M. K. Sullivan,⁶⁸ K. Suzuki,⁶⁸ S. K. Swain,⁶⁸ J. M. Thompson,⁶⁸ J. Va'vra,⁶⁸ A. P. Wagner,⁶⁸ M. Weaver,⁶⁸ C. A. West,⁶⁸ W. J. Wisniewski,⁶⁸ M. Wittgen,⁶⁸ D. H. Wright,⁶⁸ H. W. Wulsin,⁶⁸ A. K. Yarritu,⁶⁸ K. Yi,⁶⁸ C. C. Young,⁶⁸ V. Ziegler,⁶⁸ P. R. Burchat,⁶⁹ A. J. Edwards,⁶⁹ S. A. Majewski,⁶⁹ T. S. Miyashita,⁶⁹ B. A. Petersen,⁶⁹ L. Wilden,⁶⁹ S. Ahmed,⁷⁰ M. S. Alam,⁷⁰ J. A. Ernst,⁷⁰ B. Pan,⁷⁰ M. A. Saeed,⁷⁰ S. B. Zain,⁷⁰ S. M. Spanier,⁷¹ B. J. Wogland,⁷¹ R. Eckmann,⁷² J. L. Ritchie,⁷² A. M. Ruland,⁷² C. J. Schilling,⁷² R. F. Schwitters,⁷² B. W. Drummond,⁷³ J. M. Izen,⁷³ X. C. Lou,⁷³ F. Bianchi,^{74a,74b} D. Gamba,^{74a,74b} M. Pelliccioni,^{74a,74b} M. Bomben,^{75a,75b} L. Bosisio,^{75a,75b} C. Cartaro,^{75a,75b} G. Della Ricca,^{75a,75b} L. Lanceri,^{75a,75b} L. Vitale,^{75a,75b} V. Azzolini,⁷⁶ N. Lopez-March,⁷⁶ F. Martinez-Vidal,⁷⁶ D. A. Milanes,⁷⁶ A. Oyanguren,⁷⁶ J. Albert,⁷⁷ Sw. Banerjee,⁷⁷ B. Bhuyan,⁷⁷ H. H. F. Choi,⁷⁷ K. Hamano,⁷⁷ R. Kowalewski,⁷⁷ M. J. Lewczuk,⁷⁷ I. M. Nugent,⁷⁷ J. M. Roney,⁷⁷ R. J. Sobie,⁷⁷ T. J. Gershon,⁷⁸ P. F. Harrison,⁷⁸ J. Ilic,⁷⁸ T. E. Latham,⁷⁸ G. B. Mohanty,⁷⁸ H. R. Band,⁷⁹ X. Chen,⁷⁹ S. Dasu,⁷⁹ K. T. Flood,⁷⁹ Y. Pan,⁷⁹ M. Pierini,⁷⁹ R. Prepost,⁷⁹ C. O. Vuosalo,⁷⁹ and S. L. Wu⁷⁹

(BABAR Collaboration)

¹Laboratoire de Physique des Particules, IN2P3/CNRS et Université de Savoie, F-74941 Annecy-Le-Vieux, France

²Universitat de Barcelona, Facultat de Física, Departament ECM, E-08028 Barcelona, Spain

^{3a}INFN Sezione di Bari, I-70126 Bari, Italy

^{3b}Dipartimento di Fisica, Università di Bari, I-70126 Bari, Italy

⁴University of Bergen, Institute of Physics, N-5007 Bergen, Norway

⁵Lawrence Berkeley National Laboratory and University of California, Berkeley, California 94720, USA

⁶University of Birmingham, Birmingham, B15 2TT, United Kingdom

⁷Ruhr Universität Bochum, Institut für Experimentalphysik I, D-44780 Bochum, Germany

⁸University of Bristol, Bristol BS8 1TL, United Kingdom

⁹University of British Columbia, Vancouver, British Columbia, Canada V6T 1Z1

¹⁰Brunel University, Uxbridge, Middlesex UB8 3PH, United Kingdom

¹¹Budker Institute of Nuclear Physics, Novosibirsk 630090, Russia

¹²University of California at Irvine, Irvine, California 92697, USA

¹³University of California at Los Angeles, Los Angeles, California 90024, USA

¹⁴University of California at Riverside, Riverside, California 92521, USA

¹⁵University of California at San Diego, La Jolla, California 92093, USA

¹⁶University of California at Santa Barbara, Santa Barbara, California 93106, USA

¹⁷University of California at Santa Cruz, Institute for Particle Physics, Santa Cruz, California 95064, USA

¹⁸California Institute of Technology, Pasadena, California 91125, USA

¹⁹University of Cincinnati, Cincinnati, Ohio 45221, USA

²⁰University of Colorado, Boulder, Colorado 80309, USA

²¹Colorado State University, Fort Collins, Colorado 80523, USA

²²Technische Universität Dortmund, Fakultät Physik, D-44221 Dortmund, Germany

²³Technische Universität Dresden, Institut für Kern- und Teilchenphysik, D-01062 Dresden, Germany

²⁴Laboratoire Leprince-Ringuet, CNRS/IN2P3, Ecole Polytechnique, F-91128 Palaiseau, France

²⁵University of Edinburgh, Edinburgh EH9 3JZ, United Kingdom

^{26a}INFN Sezione di Ferrara, I-44100 Ferrara, Italy

^{26b}Dipartimento di Fisica, Università di Ferrara, I-44100 Ferrara, Italy

²⁷INFN Laboratori Nazionali di Frascati, I-00044 Frascati, Italy

^{28a}INFN Sezione di Genova, I-16146 Genova, Italy

^{28b}Dipartimento di Fisica, Università di Genova, I-16146 Genova, Italy

²⁹Harvard University, Cambridge, Massachusetts 02138, USA

³⁰Universität Heidelberg, Physikalisches Institut, Philosophenweg 12, D-69120 Heidelberg, Germany

- ³¹*Humboldt-Universität zu Berlin, Institut für Physik, Newtonstr. 15, D-12489 Berlin, Germany*
- ³²*Imperial College London, London, SW7 2AZ, United Kingdom*
- ³³*University of Iowa, Iowa City, Iowa 52242, USA*
- ³⁴*Iowa State University, Ames, Iowa 50011-3160, USA*
- ³⁵*Johns Hopkins University, Baltimore, Maryland 21218, USA*
- ³⁶*Laboratoire de l'Accélérateur Linéaire, IN2P3/CNRS et Université Paris-Sud 11, Centre Scientifique d'Orsay, B. P. 34, F-91898 Orsay Cedex, France*
- ³⁷*Lawrence Livermore National Laboratory, Livermore, California 94550, USA*
- ³⁸*University of Liverpool, Liverpool L69 7ZE, United Kingdom*
- ³⁹*Queen Mary, University of London, London, E1 4NS, United Kingdom*
- ⁴⁰*University of London, Royal Holloway and Bedford New College, Egham, Surrey TW20 0EX, United Kingdom*
- ⁴¹*University of Louisville, Louisville, Kentucky 40292, USA*
- ⁴²*Johannes Gutenberg-Universität Mainz, Institut für Kernphysik, D-55099 Mainz, Germany*
- ⁴³*University of Manchester, Manchester M13 9PL, United Kingdom*
- ⁴⁴*University of Maryland, College Park, Maryland 20742, USA*
- ⁴⁵*University of Massachusetts, Amherst, Massachusetts 01003, USA*
- ⁴⁶*Massachusetts Institute of Technology, Laboratory for Nuclear Science, Cambridge, Massachusetts 02139, USA*
- ⁴⁷*McGill University, Montréal, Québec, Canada H3A 2T8*
- ^{48a}*INFN Sezione di Milano, I-20133 Milano, Italy*
- ^{48b}*Dipartimento di Fisica, Università di Milano, I-20133 Milano, Italy*
- ⁴⁹*University of Mississippi, University, Mississippi 38677, USA*
- ⁵⁰*Université de Montréal, Physique des Particules, Montréal, Québec, Canada H3C 3J7*
- ⁵¹*Mount Holyoke College, South Hadley, Massachusetts 01075, USA*
- ^{52a}*INFN Sezione di Napoli, I-80126 Napoli*
- ^{52b}*Dipartimento di Scienze Fisiche, Università di Napoli Federico II, I-80126 Napoli, Italy*
- ⁵³*NIKHEF, National Institute for Nuclear Physics and High Energy Physics, NL-1009 DB Amsterdam, The Netherlands*
- ⁵⁴*University of Notre Dame, Notre Dame, Indiana 46556, USA*
- ⁵⁵*Ohio State University, Columbus, Ohio 43210, USA*
- ⁵⁶*University of Oregon, Eugene, Oregon 97403, USA*
- ^{57a}*INFN Sezione di Padova, I-35131 Padova, Italy*
- ^{57b}*Dipartimento di Fisica, Università di Padova, I-35131 Padova, Italy*
- ⁵⁸*Laboratoire de Physique Nucléaire et de Hautes Energies, IN2P3/CNRS, Université Pierre et Marie Curie-Paris6, Université Denis Diderot-Paris7, F-75252 Paris, France*
- ⁵⁹*University of Pennsylvania, Philadelphia, Pennsylvania 19104, USA*
- ^{60a}*INFN Sezione di Perugia, I-06100 Perugia, Italy*
- ^{60b}*Dipartimento di Fisica, Università di Perugia, I-06100 Perugia, Italy*
- ^{61a}*INFN Sezione di Pisa, I-56127 Pisa, Italy*
- ^{61b}*Dipartimento di Fisica, Università di Pisa, I-56127 Pisa, Italy*
- ^{61c}*Scuola Normale Superiore di Pisa, I-56127 Pisa, Italy*
- ¹*Princeton University, Princeton, New Jersey 08544, USA*
- ^{63a}*INFN Sezione di Roma, I-00185 Roma, Italy*
- ^{63b}*Dipartimento di Fisica, Università di Roma La Sapienza, I-00185 Roma, Italy*
- ⁶⁴*Universität Rostock, D-18051 Rostock, Germany*
- ⁶⁵*Rutherford Appleton Laboratory, Chilton, Didcot, Oxon, OX11 0QX, United Kingdom*
- ⁶⁶*CEA, Irfu, SPP, Centre de Saclay, F-91191 Gif-sur-Yvette, France*
- ⁶⁷*University of South Carolina, Columbia, South Carolina 29208, USA*
- ⁶⁸*Stanford Linear Accelerator Center, Stanford, California 94309, USA*
- ⁶⁹*Stanford University, Stanford, California 94305-4060, USA*
- ⁷⁰*State University of New York, Albany, New York 12222, USA*
- ⁷¹*University of Tennessee, Knoxville, Tennessee 37996, USA*
- ⁷²*University of Texas at Austin, Austin, Texas 78712, USA*
- ⁷³*University of Texas at Dallas, Richardson, Texas 75083, USA*

*Deceased.

†Now at Temple University, Philadelphia, Pennsylvania 19122, USA.

‡Now at Tel Aviv University, Tel Aviv, 69978, Israel.

§Also with Università di Perugia, Dipartimento di Fisica, Perugia, Italy.

||Also with Università di Roma La Sapienza, I-00185 Roma, Italy.

¶Now at University of South Alabama, Mobile, Alabama 36688, USA.

**Also with Università di Sassari, Sassari, Italy.

^{74a}*INFN Sezione di Torino, I-10125 Torino, Italy*^{74b}*Dipartimento di Fisica Sperimentale, Università di Torino, I-10125 Torino, Italy*^{75a}*INFN Sezione di Trieste, I-34127 Trieste, Italy*^{75b}*Dipartimento di Fisica, Università di Trieste, I-34127 Trieste, Italy*⁷⁶*IFIC, Universitat de Valencia-CSIC, E-46071 Valencia, Spain*⁷⁷*University of Victoria, Victoria, British Columbia, Canada V8W 3P6*⁷⁸*Department of Physics, University of Warwick, Coventry CV4 7AL, United Kingdom*⁷⁹*University of Wisconsin, Madison, Wisconsin 53706, USA*

(Received 22 December 2008; published 27 January 2009)

A search for the lepton flavor violating decays $\tau^- \rightarrow l^- K_S^0$ ($l = e$ or μ) has been performed using a data sample corresponding to an integrated luminosity of 469 fb^{-1} , collected with the *BABAR* detector at the SLAC PEP-II e^+e^- asymmetric energy collider. No statistically significant signal has been observed in either channel and the estimated upper limits on branching fractions are $\mathcal{B}(\tau^- \rightarrow e^- K_S^0) < 3.3 \times 10^{-8}$ and $\mathcal{B}(\tau^- \rightarrow \mu^- K_S^0) < 4.0 \times 10^{-8}$ at 90% confidence level.

DOI: 10.1103/PhysRevD.79.012004

PACS numbers: 11.30.Fs, 13.35.Dx, 14.60.Fg

In the standard model (SM), lepton-flavor-violating (LFV) decays of charged leptons are forbidden or highly suppressed even if neutrino mixing is taken into account [1–3]. Any occurrences of LFV decays with measurable branching fractions (BFs) would be a clear sign of new physics. No signal has been found in extensive searches for LFV in μ and τ decays (e.g. $\mu \rightarrow e\gamma$ [4], $\tau \rightarrow \mu\gamma$ [5–7]). However, within the bounds set by searches, some physics models that extend the SM include new sizable LFV processes. For a review, see Ref. [8]. In this paper a search for $\tau^- \rightarrow l^- K_S^0$ decays is presented [9].

The $\tau^- \rightarrow l^- K_S^0$ BF has been estimated in SM extensions with heavy singlet Dirac neutrinos [10] and in R -parity violating supersymmetric models [11]. In the first case, heavy neutrinos with large mass and large mixing with SM leptons are introduced. Because of the large number of independent angles and phases in the enlarged mixing matrix, the LFV amplitude cannot be precisely evaluated. In the large-mass limit of heavy neutrinos and keeping only the leading terms, theoretical upper bound estimations are of the order 10^{-16} and are thus out of experimental reach. In the second case, couplings of SM leptons to new particles are described using an R -parity violating superpotential. With many new complex couplings, the phenomenology is immensely richer, but at the same time less predictive. While R -parity conserving couplings can affect low-energy processes only through loops, R -parity violating contributions can appear as tree-level slepton or squark mediated processes, competing with SM contributions. So, while LFV decays are highly suppressed in the SM, they can be significantly enhanced in R -parity violating supersymmetry. The previous best experimental upper limits (ULs) for $\tau^- \rightarrow l^- K_S^0$ decay branching ratios were measured by the Belle Collaboration using a 281 fb^{-1} data sample: $\mathcal{B}(\tau^- \rightarrow e^- K_S^0) < 5.6 \times 10^{-8}$ and $\mathcal{B}(\tau^- \rightarrow \mu^- K_S^0) < 4.9 \times 10^{-8}$ at 90% confidence level [12].

The measurement described in this paper is performed using data collected by the *BABAR* detector at the PEP-II

asymmetric energy storage ring. Charged particles are detected and their momenta measured by a combination of a silicon vertex tracker (SVT), consisting of 5 layers of double-sided detectors, and a 40-layer central drift chamber (DCH), both operating in a 1.5 T axial magnetic field. Charged particle identification (PID) is provided by the energy loss in the tracking devices and by the measured Cherenkov angle from an internally reflecting ring-imaging Cherenkov detector (DIRC) covering the central region. Photons are measured, and electrons detected, by a CsI(Tl) electromagnetic calorimeter (EMC). The EMC is surrounded by an instrumented flux return (IFR). The detector is described in detail elsewhere [13,14].

The analyzed data sample corresponds to an integrated luminosity of 469 fb^{-1} collected from e^+e^- collisions, 425 fb^{-1} at the $Y(4S)$ resonance and 44 fb^{-1} at center-of-mass (CM) energy 10.54 GeV. The total number of produced τ pairs $N_{\tau\tau}$ is $(4.31 \pm 0.03) \times 10^8$, calculated using the average τ cross section of $0.919 \pm 0.003 \text{ nb}$ estimated with KK2f [15]. The Monte Carlo (MC) simulated samples of τ leptons are produced using the KK2f generator [16,17] and Tauola decay library [18,19]. Decays of B mesons are simulated with the EvtGen generator [20], while $e^+e^- \rightarrow q\bar{q}$ events, where $q = u, d, s$ quarks (referred to as uds events) or $q = c$ quark, are simulated with the JETSET generator [21]. The *BABAR* detector is modeled in detail using the GEANT4 simulation package [22]. Radiative corrections for signal and background processes are simulated using PHOTOS [23]. In the following, the simulated signal and background samples will be referred to as signal MC and background MC samples, respectively.

For this analysis, two different stages of selection are used. In the first, which we call the loose selection stage, we retain enough data to estimate background distribution shapes. The second, which we refer to as the tight selection, uses criteria that have been chosen to optimize the sensitivity. The sensitivity, or expected UL, is defined as the UL value obtained using the background expected from MC: we choose selection criteria that give the smallest

expected UL. We use loose and tight electron and muon PID selectors for the two stages of selection. The selectors are based on combinations of measurements from the various subdetectors. The average efficiency for the loose electron (muon) selector is 98% (92%) for a laboratory momentum $p_{\text{LAB}} > 0.6(1.4)$ GeV/ c , whereas the π misidentification rate is less than 10% (6%). The average identification efficiency for the tight electron (muon) selector with a likelihood based algorithm is 93% (80%) for the same momentum range, whereas the π misidentification rate is less than 0.1% (2%). All selection criteria are applied to both channels and quantities are defined in the CM system, unless stated otherwise.

Events are first selected using global event properties in order to reject $b\bar{b}$, $c\bar{c}$, and uds background events with high multiplicity. All tracks (photons) are required to be reconstructed within a fiducial region defined by $0.410 < \theta < 2.540$ ($0.410 < \theta < 2.409$) radians, where θ is the polar angle in the laboratory system with respect to the z axis direction [13]. The overall event charge must be zero. Furthermore, the event must include a K_S^0 candidate with an invariant mass within 25 MeV/ c^2 of the nominal K_S^0 mass [24], reconstructed from two oppositely charged tracks, assuming the pion mass for both. The highest momentum track in the CM frame has to have a momentum between 1.5 and 4.8 GeV/ c for both modes. For the electron channel events, the total EMC energy associated with tracks in the laboratory frame has to be less than 9 GeV. The thrust [25] is calculated using tracks and calorimeter energy deposits without an associated charged particle track. The thrust magnitude has to be between 0.85 (0.88) and 0.98 (0.97) for the electron (muon) channel. For each event, two hemispheres are defined in the CM frame using the plane perpendicular to the thrust axis. The hemisphere that contains the reconstructed τ candidate, defined below, is referred to as the signal side and the other hemisphere as the tag side. Candidate τ pair events are required to have three reconstructed charged particle tracks on the signal side. On the tag side, one track only is required for the muon channel, while for the electron channel, events with one or three reconstructed tracks are retained.

The signal τ candidates are reconstructed by combining one K_S^0 candidate with the third track of the signal hemisphere, to which mass is assigned according to the considered decay mode. The lepton track is required to be identified as an electron or muon by the loose PID selector. The signal τ candidates are then examined in the two dimensional distribution of ΔE_τ vs ΔM_τ , where ΔM_τ is defined as the difference between the invariant mass of the reconstructed τ and the world average value [24], and ΔE_τ is defined as the difference between the energy of the reconstructed τ and the expected τ energy, half the CM total energy. Only τ candidates with a ΔM_τ value within ± 0.35 GeV/ c^2 and a ΔE_τ value within ± 0.4 GeV are retained. The whole decay tree is then fitted requiring

that, within reconstruction uncertainties, the K_S^0 decay products form a vertex, the K_S^0 mass is constrained to the nominal value, and the track and the K_S^0 trajectory form a vertex close to the beam interaction region. To improve the energy resolution, a bremsstrahlung recovery procedure is applied for the $\tau^- \rightarrow e^- K_S^0$ decay mode only: before the fit, the e^- track candidate is combined with up to three photons with an energy larger than 30 MeV and contained in a cone around the track direction of $\Delta\theta \times \Delta\phi = 0.035 \times 0.050$ rad 2 , where θ is the polar angle and ϕ the azimuthal angle in the laboratory system. The constrained fit must have a χ^2 probability larger than 1%. If more than one candidate is found (which occurs in less than 1% of the events), only that with the largest χ^2 probability is retained.

After the above selection is applied, backgrounds remain, mainly from Bhabha events for the electron channel and from nonlepton events for the muon channel due to the larger pion to muon misidentification. To improve the background rejection, further requirements are imposed on the K_S^0 candidates. For the muon channel, the K_S^0 laboratory momentum must be greater than 1.0 GeV/ c . For the electron channel, in order to remove events with a photon conversion faking a K_S^0 , the invariant mass of the K_S^0 daughters, calculated using the momentum from the fit and assigning them the electron mass, is required to be greater than 0.10 GeV/ c^2 . The K_S^0 flight length significance is computed as the three-dimensional distance in the laboratory system between the τ vertex and the K_S^0 vertex, divided by its error, and we select events with a flight length significance greater than 3.0. Finally, the K_S^0 reconstructed mass is required to be between 0.482 and 0.514 GeV/ c^2 . The last two criteria are included in the loose selection for the electron channel while, for the muon channel, they are applied at a later stage in order to maintain sufficient statistics in the loose selection sample. The amount of background events due to dimuon and Bhabha processes is negligible after the loose selection has been applied and most of the surviving events come from charm decays, such as $D^- \rightarrow K_S^0 \pi^-$ and $D^- \rightarrow K_S^0 \ell^- \nu$, and from combinations in the uds events of a true K_S^0 and a fake lepton.

To avoid bias from adapting selection requirements to the data, the tight selection has been optimized in a blind way, without looking at the data in the rectangular region (blinded box) shown in Fig. 1, corresponding to more than ± 5 times the resolution for signal events on ΔE_τ and ΔM_τ , respectively. As discussed above, selection criteria have been chosen to optimize the sensitivity on the upper limit. Therefore, for the tight selection the tighter PID selectors plus the following requirements are applied. The event's missing momentum is computed by subtracting from the e^+e^- momentum all track candidates and all unmatched calorimeter energy deposits. To reject events with tracks and photons lost out of the acceptance, the missing mo-

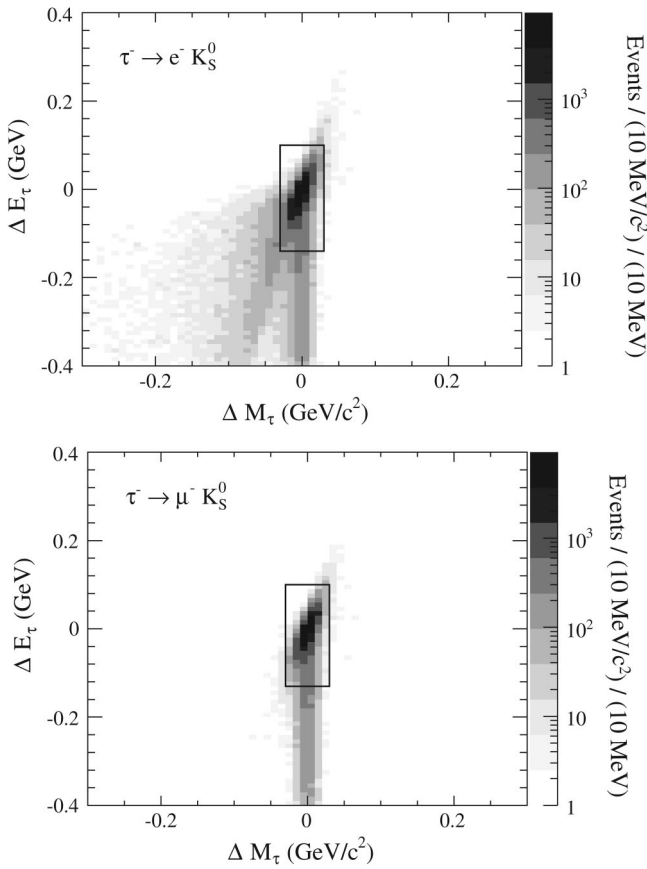


FIG. 1. Candidate distributions for signal MC samples $\tau^- \rightarrow e^- K_S^0$ (top) and $\tau^- \rightarrow \mu^- K_S^0$ (bottom) in the $(\Delta E_\tau, \Delta M_\tau)$ plane after the loose selection. The rectangle corresponds to the blinded box. The z -axis scale is logarithmic.

momentum is required to have a transverse component greater than 0.1(0.2) GeV/ c for the electron (muon) channel and the cosine of its polar angle in the laboratory system must be smaller than 0.95. In a τ pair event, when neglecting radiation, the tag-side τ has the same momentum as the signal-side τ but the opposite direction. In addition, assuming that the tag τ decays to a one neutrino (hadronic) mode, the event's missing momentum corresponds to the neutrino momentum. These two assumptions determine the tag τ 4-momentum \hat{p}_{TAG} , and the neutrino 4-momentum \hat{p}_ν , respectively, and we define the squared invariant mass m_{TAG}^2 as $(\hat{p}_{\text{TAG}} - \hat{p}_\nu)^2$. As shown in Fig. 2, m_{TAG}^2 peaks at small values for signal events and extends to higher values for background events. The tail on the right for the signal sample is due to tag τ decays to (leptonic) modes with two neutrinos, while the tail on the left for the background sample is due to events with missing energy from lost photons or tracks. The variable m_{TAG}^2 is required to be smaller than 2.6 (GeV/ c^2) 2 for both channels. Shapes for data and MC agree within error but a discrepancy is observed in the normalization. This does not affect the results because the final number of background events is

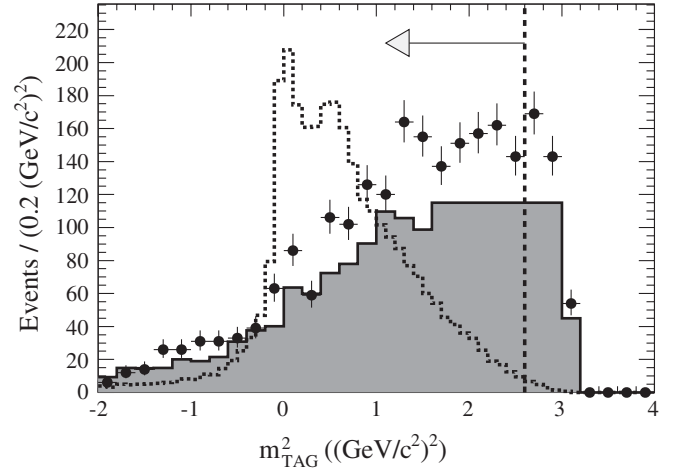


FIG. 2. Distributions of m_{TAG}^2 after the loose selection for the $\tau^- \rightarrow e^- K_S^0$ channel. The data distribution is shown by solid circles with error bars, background MC with a filled histogram and signal MC with a dashed line. The signal MC distribution is normalized arbitrarily, while the background MC is normalized to the data luminosity. The vertical dashed line and the arrow indicate the applied requirement.

obtained using the data sample. The uds background events are further reduced by requiring less than six photons on the tag side. Signal events have missing momentum due only to the undetected neutrino(s) from the tagging τ decay. Therefore, only for the $\tau^- \rightarrow \mu^- K_S^0$ channel, the cosine of the angle between the missing momentum and the signal τ candidate is required to be negative, to further reject nonleptonic backgrounds and improve the sensitivity.

For the final step of analysis, we define another discriminating variable, χ_{FULL}^2 , as the χ^2 of the geometrical and kinematical fit for the whole decay tree, with additional constraints of ΔM_τ and ΔE_τ equal to 0. Most signal events have χ_{FULL}^2 values in the range 0–50, and we consider this range in the following. In Fig. 3 we show the distributions of χ_{FULL}^2 for data and signal MC inside the blinded box after the tight selection. An analytic curve describing the background, as detailed in the following, is also presented. The overall efficiency ε in this range of χ_{FULL}^2 , after the tight selection, and inside the blinded box is 9.4% for the $\tau^- \rightarrow e^- K_S^0$ mode and 7.0% for the $\tau^- \rightarrow \mu^- K_S^0$ mode. The total signal efficiency is estimated by dividing the number of selected signal MC events by the total number of generated $\tau^- \rightarrow l^- K_S^0$ decays and includes the $K_S^0 \rightarrow \pi^+ \pi^-$ BF.

We estimate the number of background events in the signal region using the number of MC background events in the range 0–50 of χ_{FULL}^2 after the loose selection multiplied by the ratio of numbers of MC background events after tight and loose selections in the full range of χ_{FULL}^2 . We apply a 10% correction to normalize the MC to the levels of background seen in data outside the blinded box

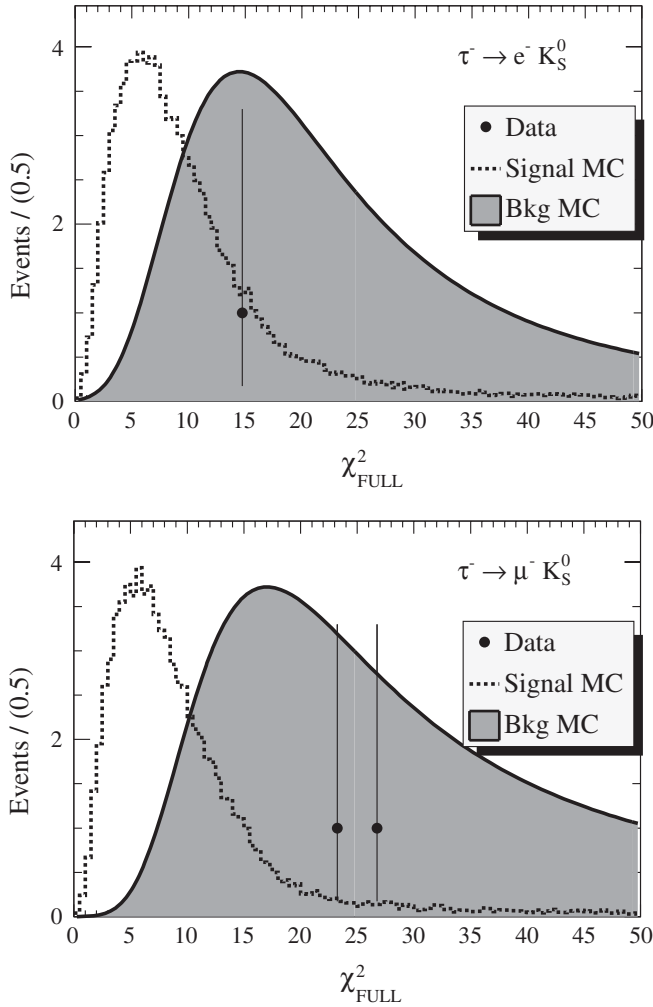


FIG. 3. Distributions of χ^2_{FULL} after the tight selection for the $\tau^- \rightarrow e^- K_S^0$ (top) and $\tau^- \rightarrow \mu^- K_S^0$ (bottom) channel. The data events are shown by solid circles with error bars. The signal MC distributions are shown by dashed lines, while the background shapes are shown with filled histograms. The signal and background MC distributions are normalized arbitrarily.

after the tight selection. Total backgrounds of 1.0 ± 0.4 and 5.3 ± 2.2 events are expected for $\tau^- \rightarrow e^- K_S^0$ and $\tau^- \rightarrow \mu^- K_S^0$ respectively. Finally, the signal region is unblinded and 1 and 2 events are found for electron and muon modes, respectively, as already shown in Fig. 3.

Since no excess above the expected background level is found, 90% confidence level limits have been determined according to the modified frequentist analysis (or CL_S method) [26,27]. This method is more powerful than a simple UL estimation based on numbers of observed and expected events as it takes into account the different distributions of one or more discriminating variables between signal and background. The discriminating variable used in this analysis is χ^2_{FULL} . The signal χ^2_{FULL} distribution is simply provided by the MC sample as already shown in Fig. 3, but this cannot be done for the background as too few events survive the tight selection, but also the loose

one. Therefore we obtain smooth background shapes by fitting the product of a Landau function and a straight line to the MC background distributions after the loose selection. Any distortions on the shapes that could be introduced by the tight selection are negligible compared to the uncertainties of the shapes themselves. The resulting curves are presented in Fig. 3. The adopted test-statistic is the likelihood ratio $Q = \mathcal{L}(S+B)/\mathcal{L}(B)$, where $\mathcal{L}(B)$ and $\mathcal{L}(S+B)$ are, respectively, the likelihood to find the observed events in the hypothesis of background only and of background plus a given amount of signal. The latter, and consequently Q , are functions of the hypothesized signal BF. The confidence level CL_S is defined as the ratio CL_{S+B}/CL_B , where CL_{S+B} and CL_B are estimated using an ensemble of simulated data sets, generated from signal plus background or background only. The generation is iterated with a varying hypothetical value of the number of signal events, depending on the BF. CL_{S+B} and CL_B are then the probabilities that the test-statistic would be less than the Q_{exp} values observed in data, under the respective hypothesis. Signal hypotheses corresponding to $CL_S < \alpha$ are rejected at the $1 - \alpha$ confidence level. This method avoids that a negative fluctuation of the background is translated into a large improvement of the exclusion limit and allows to include uncertainties directly on signal and background distributions. The ULs on BFs at 90% confidence level are calculated as

$$\mathcal{B}(\tau^- \rightarrow l^- K_S^0) < \frac{s_{90}}{2\varepsilon N_{\tau\tau}}, \quad (1)$$

where s_{90} is the limit for the signal yield at 90% confidence level, and ε and $N_{\tau\tau}$ are already defined above. The dominant systematic uncertainties on the signal efficiency for the electron (muon) channel come from possible data/MC differences in the efficiency of the PID requirements, 0.4% (5.1%) and of the tracking reconstruction, 1.7% (1.6%). Other sources of systematic uncertainty for the efficiency are: data/MC differences in K_S^0 reconstruction efficiency (1.0%), the beam energy scale and the energy spread (less than 0.2%). The efficiency errors from MC statistics are negligible compared with the systematics ones. The uncertainty for the total number of τ pairs comes from the error on the luminosity and on the τ cross section values (0.7%). We assume these uncertainties are uncorrelated and combine them in quadrature to give a total signal uncertainty of 2.1% and 5.5%, respectively, for the electron and muon channels. For each bin of the signal χ^2_{FULL} distribution, we consider the total uncertainties on the signal yield, and for the background distributions the uncertainties on the expected background levels. The uncertainties are treated as fully correlated between the bins as they are mainly due to normalization uncertainties. The analysis results are summarized in Fig. 4 presenting CL_S for the observed events versus the BFs, with the horizontal line defining the UL at 90% confidence level.

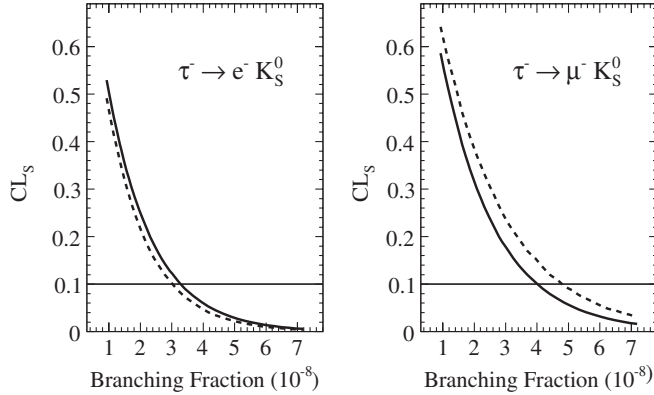


FIG. 4. Observed (full line) and expected (dashed line) CL_S as a function of the BFs (10^{-8}) for the decays $\tau^- \rightarrow e^- K_S^0$ and $\tau^- \rightarrow \mu^- K_S^0$.

From Fig. 4, the ULs on the BFs at 90% confidence level are determined to be: $\mathcal{B}(\tau^- \rightarrow e^- K_S^0) < 3.3 \times 10^{-8}$ and $\mathcal{B}(\tau^- \rightarrow \mu^- K_S^0) < 4.0 \times 10^{-8}$. The CL_S obtained using the number of expected background MC events, instead of data, are shown in the same figure and the BF values at 90% confidence level can be regarded as the sensitivities: 3.0×10^{-8} for the electron channel and 4.8×10^{-8} for the muon one.

ULs are also determined by exploiting another technique that gives a similar but worse sensitivity for the UL, so it is used only as a cross-check. For this method, selection criteria on the same quantities were slightly tightened to reduce the background as much as possible, and signal candidates are counted inside the elliptical region shown in Fig. 5. The final signal efficiencies with these selections are 9.1% for the $\tau^- \rightarrow e^- K_S^0$ mode and 6.1% for the $\tau^- \rightarrow \mu^- K_S^0$ mode. The level of background in the signal ellipse

is estimated by extrapolating the event densities found in two sideband regions of ΔM_τ , as defined in Fig. 5. The ΔM_τ background distribution is modeled as a linear function plus a Gaussian function to account for the peak related to the decay mode $D^- \rightarrow K_S^0 \pi^-$. This is fitted at the loose selection stage, where there are sufficient statistics in the sidebands to estimate the shape. Then the fitted background distribution is normalized according to the number of data events in the sidebands after the tight selection. The final estimated number of background events in the signal region is $0.59 \pm (0.19 \oplus 0.17)$ and $0.30 \pm (0.17 \oplus 0.05)$ for the electron and muon channels, respectively, where the last number is the systematic uncertainty accounting for the observed differences between estimated and real MC sample events inside the signal region at the loose selection stage. When the signal region is unblinded, we find inside the elliptical signal region only one event for each channel. Using the signal efficiencies, the estimated residual backgrounds, and the number of observed events ULs on the BFs at 90% confidence level for this cross-check are calculated with the POLE program [28]. Uncertainties are included assuming that efficiency and background values have a Gaussian distribution, and that they are not correlated. The resulting ULs are $\mathcal{B}(\tau^- \rightarrow e^- K_S^0) < 4.8 \times 10^{-8}$ and $\mathcal{B}(\tau^- \rightarrow \mu^- K_S^0) < 7.6 \times 10^{-8}$.

In conclusion, a search for the lepton flavour violating decays $\tau^- \rightarrow l^- K_S^0$ has been performed using a data sample of 469 fb^{-1} collected with the *BABAR* detector at the SLAC PEP-II electron-positron storage rings. No statistically significant excess of events is observed in either channel and the resulting ULs are $\mathcal{B}(\tau^- \rightarrow e^- K_S^0) < 3.3 \times 10^{-8}$ and $\mathcal{B}(\tau^- \rightarrow \mu^- K_S^0) < 4.0 \times 10^{-8}$ at 90% confidence level. These results are the most restrictive ULs on the BFs of these decay modes, and can be used to constrain

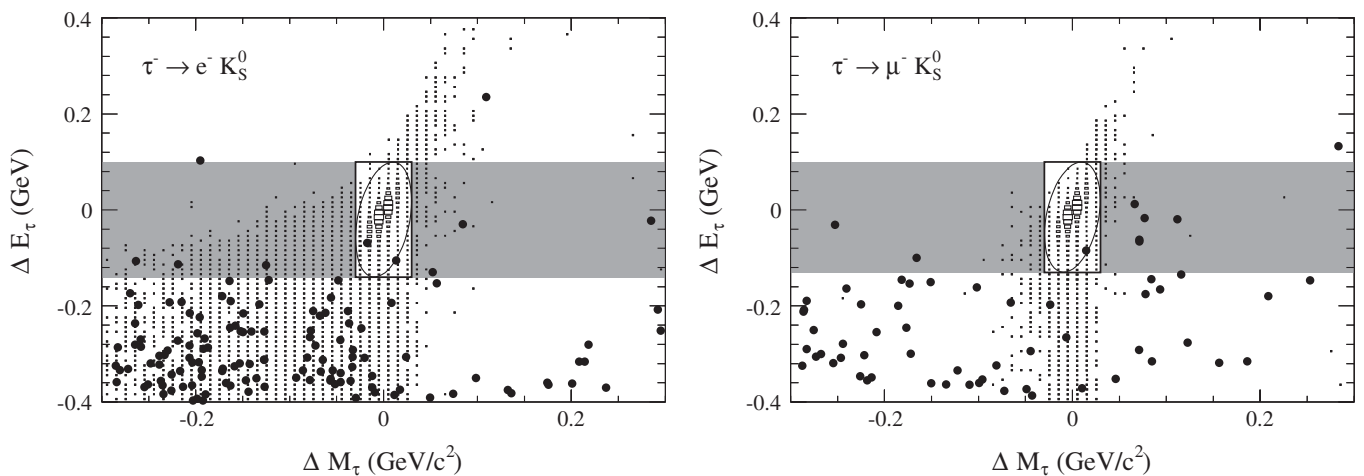


FIG. 5. Candidate distribution in the $(\Delta E_\tau, \Delta M_\tau)$ plane after all selections for cross-check method ($\tau^- \rightarrow e^- K_S^0$ on the left, $\tau^- \rightarrow \mu^- K_S^0$ on the right). Data candidates are indicated by solid circles. The boxes show the signal MC distribution with arbitrary normalization. The blinded box, used for both methods, corresponds to the rectangle. The gray bands and the ellipse indicate the sidebands used for extrapolating the background and the signal region for the cross-check measurement. The z -axis scale is linear.

parts of the theoretical phase space in several models of physics beyond the standard model.

We are grateful for the extraordinary contributions of our PEP-II colleagues in achieving the excellent luminosity and machine conditions that have made this work possible. The success of this project also relies critically on the expertise and dedication of the computing organizations that support *BABAR*. The collaborating institutions wish to thank SLAC for its support and the kind hospitality extended to them. This work is supported by the US Department of Energy and National Science Foundation, the Natural Sciences and Engineering Research Council (Canada), the Commissariat à l’Energie Atomique and

Institut National de Physique Nucléaire et de Physique des Particules (France), the Bundesministerium für Bildung und Forschung and Deutsche Forschungsgemeinschaft (Germany), the Istituto Nazionale di Fisica Nucleare (Italy), the Foundation for Fundamental Research on Matter (The Netherlands), the Research Council of Norway, the Ministry of Education and Science of the Russian Federation, Ministerio de Educación y Ciencia (Spain), and the Science and Technology Facilities Council (United Kingdom). Individuals have received support from the Marie-Curie IEF program (European Union) and the A. P. Sloan Foundation.

-
- [1] W.J. Marciano and A.I. Sanda, Phys. Lett. **67B**, 303 (1977).
- [2] B. W. Lee and R. E. Shrock, Phys. Rev. D **16**, 1444 (1977).
- [3] T.-P. Cheng and L.-F. Li, Phys. Rev. D **16**, 1425 (1977).
- [4] M.L. Brooks *et al.* (MEGA Collaboration), Phys. Rev. Lett. **83**, 1521 (1999).
- [5] B. Aubert *et al.* (*BABAR* Collaboration), Phys. Rev. Lett. **95**, 041802 (2005).
- [6] B. Aubert *et al.* (*BABAR* Collaboration), Phys. Rev. Lett. **96**, 041801 (2006).
- [7] K. Hayasaka *et al.* (Belle Collaboration), Phys. Lett. B **666**, 16 (2008).
- [8] M. Raidal *et al.*, Eur. Phys. J. C **57**, 13 (2008).
- [9] Charge conjugate decays are implicitly included.
- [10] A. Ilakovac, Phys. Rev. D **62**, 036010 (2000).
- [11] J.P. Saha and A. Kundu, Phys. Rev. D **66**, 054021 (2002).
- [12] Y. Miyazaki *et al.* (Belle Collaboration), Phys. Lett. B **639**, 159 (2006).
- [13] B. Aubert *et al.* (*BABAR* Collaboration), Nucl. Instrum. Methods Phys. Res., Sect. A **479**, 1 (2002).
- [14] W. Menges, IEEE Nucl. Sci. Symp. Conf. Rec. **5**, 1470 (2006).
- [15] S. Banerjee, B. Pietrzyk, J.M. Roney, and Z. Was, Phys. Rev. D **77**, 054012 (2008).
- [16] S. Jadach, B.F.L. Ward, and Z. Was, Comput. Phys. Commun.. **130**, 260 (2000).
- [17] B.F.L. Ward, S. Jadach, and Z. Was, Nucl. Phys. B, Proc. Suppl. **116**, 73 (2003).
- [18] S. Jadach, Z. Was, R. Decker, and J.H. Kuhn, Comput. Phys. Commun. **76**, 361 (1993).
- [19] E. Barberio and Z. Was, Comput. Phys. Commun. **79**, 291 (1994).
- [20] D.J. Lange, Nucl. Instrum. Methods Phys. Res., Sect. A **462**, 152 (2001).
- [21] T. Sjostrand, S. Mrenna, and P. Skands, J. High Energy Phys. 05 (2006) 026.
- [22] S. Agostinelli *et al.* (GEANT Collaboration), Nucl. Instrum. Methods Phys. Res., Sect. A **506**, 250 (2003).
- [23] P. Golonka *et al.*, Comput. Phys. Commun. **174**, 818 (2006).
- [24] W.M. Yao *et al.* (Particle Data Group Collaboration), J. Phys. G **33**, 1 (2006).
- [25] S. Brandt, C. Peyrou, R. Sosnowski, and A. Wroblewski, Phys. Lett. **12**, 57 (1964).
- [26] T. Junk, Nucl. Instrum. Methods Phys. Res., Sect. A **434**, 435 (1999).
- [27] *Workshop on Confidence Limits, CERN, Geneva, Switzerland, 2000: Proceedings* (CERN Report No. 2000-005, 2000).
- [28] J. Conrad, O. Botner, A. Hallgren, and C. Perez de los Heros, Phys. Rev. D **67**, 012002 (2003).